Coastal Dynamics 2017
Paper No. 192

CHARACTERISTICS AND DYNAMICS OF CRESCENTIC BAR EVENTS IN AN OPEN, TIDELESS BEACH

Rinse de Swart[1], Francesca Ribas[1], Gerben Ruessink[2], Gonzalo Simarro[3] and Jorge Guillén[3]

Abstract

Crescentic bar events at Castelldefels beach (NW Mediterranean) have been characterised using a 4.25 years dataset (October 2010-December 2014) of time-exposure video images. Crescentic bars are observed during 41% of the study period, with an irregular distribution of the events in the different years. The crescentic bars have a lifetime that varies from 1 to over 100 days, a mean wavelength of 245 m and a mean amplitude of 9 m. The bars are observed in relatively low-energetic wave conditions with a wide variety of wave angles. The formation of crescentic bars also depends on the antecedent bathymetry, in particular crescentic bar events only occur when the sandbar is located at least at 50 m from the shoreline. Crescentic bar destruction at Castelldefels beach is observed in both low- and high energetic wave conditions, but the angle of incidence is always oblique.

Key words: nearshore morphodynamics, Castelldefels beach, bar events, video observations, crescentic bars

1. Introduction

In the nearshore zone of many beaches around the globe, one or several shore-parallel sand bars are often present where incoming waves predominately break. These sand bars are dynamic and change their shape regularly as a result of variations in wave conditions. Generally, the morphology of shore-parallel sand bars varies from alongshore continuous ridges (linear bars) through regular undulating sequences of shallower and deeper sections (meandering bars) to little-relief terrace-shaped bars (King and Williams, 1949; Wright and Short, 1984, van Enckevort et al., 2004; and others). Meandering bars are often referred to as crescentic bars (and/or rip and channel systems) and they usually feature undulations with distinct crescent moons where the horns (shallow areas) point shoreward and the bays (deeper regions) are located seaward (Ribas et al., 2015). Nowadays, it is widely accepted that crescentic bars develop due to self-organization mechanisms (Ribas et al., 2015). Waves that break over the shallow areas of crescentic horns generate lateral flows that converge creating strong rip currents that flow seaward through the deeper parts, called rip channels. The corresponding sediment transport produces accretion on the horns and erosion on the channels, thus creating a positive feedback between wave-driven currents and the morphology ('bed surf instability', see Calvete et al., 2005).

Crescentic sand bars have been studied intensively during the last decades, resulting in a relatively good knowledge of their formation mechanism, their morphological characteristics and their dynamics (Price and Ruessink, 2011; Garnier et al., 2013; Contardo and Symonds, 2015; and references therein). Crescentic bars develop when beaches advance through an accretionary (downstate) sequence (Short, 1979), that may take several days up to a few weeks (van Enckevort et al., 2004). On the contrary, crescentic bar straightening occurs during an erosional (upstate) sequence, which often lasts less than one day. An erosional sequence in which all pre-existing alongshore-variable morphology is wiped out and an

[1] Physics Department, Universitat Politècnica de Catalunya, Barcelona, Spain. rinse.deswart@planet.nl ; francesca.ribas@upc.edu
[2] Department of Physical Geography, Faculty of Geosciences, Utrecht University, Utrecht, the Netherlands. b.g.ruessink@uu.nl
[3] Department of Marine Geosciences, Institut de Ciències del Mar (ICM-CSIC), Barcelona, Spain. simarro@icm.csic.es ; jorge@icm.csic.es

alongshore-uniform bar develops is often referred to as a morphological reset. Traditionally, the transitions from a shore-parallel bar to a crescentic bar and vice versa were associated to the amount of incoming wave energy, with bar straightening occurring for high energy waves (Lippmann and Holman, 1990; van Enckevort and Ruessink, 2003; Ranasinghe et al., 2004). However, more recent observational studies (Holman et al., 2006; Price and Ruessink, 2011; Contardo and Symonds, 2015) found the angle of incidence of particular importance. These studies indicated that crescentic bars primarily develop for normal wave incidence and morphological resets occur in both intermediate- and high-energy wave conditions, but only if the waves are obliquely incident. Moreover, these studies emphasized that high-energy wave conditions are not necessary for morphological resets. Garnier et al. (2013) suggested that bar straightening results from a weakening of the bed-surf mechanism in case of oblique waves, leading to a negative feedback between currents and the morphology.

Still, the role of wave obliquity in crescentic bar formation and destruction is not yet clear, and processes such as splitting and merging of individual crescents and crescentic bar coupling with megacusps deserve further attention. Also, there is a lack of crescentic bar observations in fetch-limited environments with insignificant tides, where waves are the only existing morphodynamic forcing, such as Mediterranean beaches. This paper aims to further our understanding of the dynamics of crescentic bars (including straightening) at Mediterranean beaches. This will be done by using a 4.25 years-long dataset of daily high-quality video images from Castelldefels beach, Catalunya, Spain (Section 2). The methods used to characterise the crescentic bar events are explained in Section 3. Subsequently, the different crescentic bar events are quantified and correlated to the wave conditions, paying special attention to the formation and destruction of the crescentic bar (Section 4). Finally, section 5 compares the main findings of this study with previous research and the most important outcomes of this study are listed in Section 6.

2. Study area and data collection

2.1. *Study area*

The study site is Castelldefels beach, an open, dissipative beach located approximately 20 km southwest of Barcelona (Northeast Spain), at the Western Mediterranean Sea. Tidal action in this part of the Mediterranean Sea is very small, with a tidal range of approximately 40 (20) cm during spring tide (neap tide), so that it is considered a tideless beach (Simarro et al., 2015). Castelldefels beach is approximately 4.5 km long and is part of a continuous stretch of beaches of the Llobregat delta, extending from the Garraf Mountain chain in the west to the Llobregat river outfall in the east. The orientation of Castelldefels beach is east-west and the study site is located in its eastern part (41°15'54.7"N, 1°59'29.1"E) and extends over an alongshore distance of 1 km. The beach is mainly composed of sand with a median grain size of 270 μm.

2.2. *Morphologic data*

At Castelldefels beach, a video monitoring system operates since 5 October 2010. The video system is installed in a 30-m-high observation tower and consists of 5 full-colour cameras that cover a 180º overview of the shoreline. The system uses the SIRENA open source code (Nieto et al., 2010). Each daylight hour, all the cameras produce one snapshot, one time-exposure and one variance image. The size of the images is of 1280 × 960 pixels. Each time-exposure image is produced by averaging numerous instantaneous snap-shots during a 10-min period, showing clear stripes of foam, which in turn indicates the location of the submerged sand bars. Finally, the time-exposure images from the 5 cameras are georeferenced, rectified and merged into a planview of the shoreline with a pixel resolution of 0.5 m and a size of 2001 × 601 pixels or 1000 by 300 m (e.g., Figure 1, up) using the ULISES open source code (Simarro et al., 2017). The origin of the coordinate system in the planviews is the location of the camera system (41°15'54.7"N, 1°59'29.1"E). The time period studied in the present contribution spans from 5 October 2010 to 31 December 2014. During this period of 1549 days, a nearly uninterrupted dataset of images is available with only 69 days without any images.

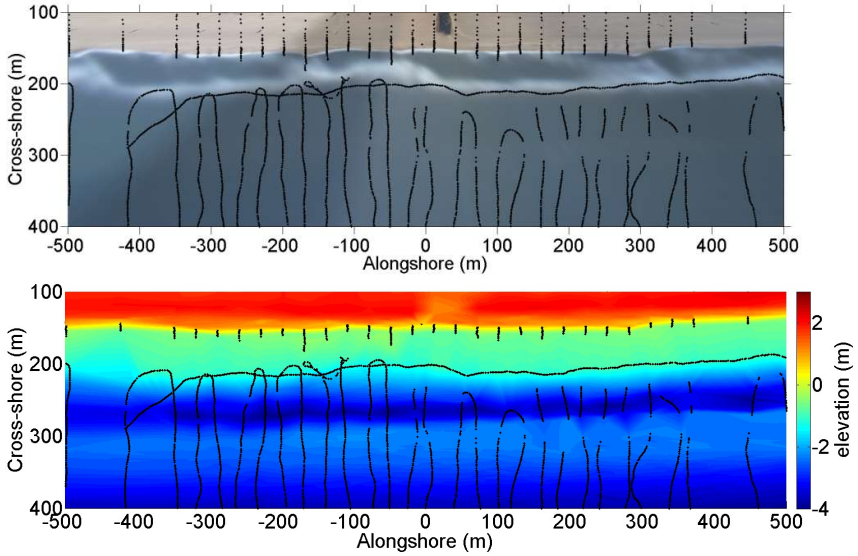

Figure 1: (Up) Example of a planview image on 24 April 2013, with a crescentic bar of some 400 m wavelength. The white areas indicate locations with dominant wave breaking. (Down) Bathymetric survey at Castelldefels beach on 24 April 2013. The same coordinate system is used in both images. The black lines in both images indicate the locations where the bathymetric measurements were taken.

During the study period, a total of six bathymetric surveys were conducted at Castelldefels beach: 8 December 2011, 1 June 2012, 8 October 2012, 23 April 2013, 9 October 2013 and 3 May 2014. The surveys comprise the dry beach and the submerged bathymetry over 1700 m offshore, up to a depth of over 20 m (e.g., Figure 1, down). However, bathymetric measurements were not performed in the inner surf zone (from z = -0.5 m to z = -1.5 m, approximately) so that it is not possible to use them directly to measure the bar crest locations. The three latter surveys indicate the presence of an inner bar, which might be a terrace because its landward side is not measured, and all of them show an outer bar. In 2011 and 2012, the inner bar is not visible on the surveys and the outer bar is located around the cross-shore coordinate x = 240 – 260 m. In 2013 the inner bar is already visible at about x = 180 – 200 m, whilst the outer bar is located around x = 300 m (e.g., Figure 1, down). In 2014, the inner bar remains at about the same cross-shore position whilst the outer bar is situated around cross-shore coordinate x = 320 m.

2.3. *Wave data*

For this study, hourly values of the root-mean-square wave height H_{rms}, peak period T_p and incidence angle θ were obtained from the SIMAR model point 2108135, located in front of the Castelldefels coast. Although an offshore wave buoy (Boya Barcelona II) is also located relatively close to the study site, we decided not to use the data of this buoy because not all wave directions that are important at Castelldefels beach can be registered properly by the buoy (waves from the west-southwest cannot easily reach the buoy due to sheltering). The data from the wave buoy and from the SIMAR point 712018020, which is located directly next to the wave buoy, were previously compared in order to validate the SIMAR dataset. The used SIMAR model point 2108135 is located at deep water (at a depth of approximately 70 m) and the waves were propagated to a depth of 10 m using Snell's law, dispersion relation and wave energy conservation (linear wave theory). The angle of incidence is defined with respect to the shore normal, where positive (negative) angles indicate that waves come from the west (east).

The open beach of Castelldefels is exposed to waves throughout the year (Figure 2). The long-term average values of H_{rms}, T_p and absolute θ during the entire study period (at 10 m depth) are 0.32 m, 4.4 s and 35°

respectively. Higher than average spectral wave heights are predominantly observed between September and March, corresponding to the autumn and winter period. The wave climate at Castelldefels is characterised by waves from both the East-Southeast and the Southwest. The highest waves in this part of the Catalan coastline come from the East, due to the largest available fetches and the stronger winds that generally blow from this direction (Sánchez-Arcilla et al., 2008; Bolaños et al., 2009).

3. Methods

During the entire study period, a visual analysis of the time-exposure planview images around 12:00 midday was performed. This time was chosen because the sun is high in the sky and not much sun glare in the images occurs. The visual analysis focused on tracking the visibility of the inner and outer bar, and also the occurrence of crescentic bar events, their duration and the date of formation and destruction. The inner bar was visible during most of the study period and only became invisible under very low energetic wave conditions, whilst the outer bar was only visible a few days each year during storm conditions.

A crescentic bar event was defined as that in which at least 2 undulations could be visually distinguished for at least one full day. These events were then further subdivided into 'developed events' and 'well-developed events'. The well-developed events should last for at least 3 consecutive days and the cross-shore distance between the bays and horns should be at least 15 m. Moreover, particular attention was paid to formation and destruction moments of the crescentic bar events. Formation moments were defined as the moment when the first clear crescentic pattern was visible in the planview images, following a period with only shore-parallel bars. Similarly, destruction moments were defined as the moment when a crescentic pattern was not visible anymore in the planview images, following a period with only crescentic bars. These were further subdivided in 'unclear destruction/formation' (when, e.g., no images were available during destruction/formation) and 'clear destruction/ formation'.

The barlines in the planview images were tracked using the so called BarLine Intensity Mapper (BLIM), a tool that incorporates the algorithm of van Enckevort and Ruessink (2001), which detects the maximum intensity value in a cross-shore transect, and is a proxy of the shallowest point in the underlying bathymetry (bar crest). First, the best planview image (e.g., with foam presence, minimum sun glare, etc.) per day was selected to further quantify the bar characteristics. In case large changes in the wave breaking pattern were observed on the same day, up to three images per day were used. Days that only contained images without a clear wave breaking pattern (low energetic conditions) or low-quality images (due to, e.g., sun glare or darkness) were discarded from the analysis. Second, for each selected image, the cross-shore location of the intensity peaks was inferred for each alongshore location using BLIM, resulting in a smoothed barline, The alongshore varying pattern in the barline reflects the presence of bays (seaward perturbations) and horns (shoreward perturbations) that are characteristic of crescentic bars. Applying this procedure to all images in the dataset leads to a matrix $B(t,y)$, that contains cross-shore bar crest positions B at time t and alongshore position y. The average alongshore sandbar position $B_y(t)$ was also computed.

For some time periods, a more detailed analysis of the crescentic bars was performed. First, the bays and horns in each detrended barline were detected, ensuring that the cross-shore distance between a consecutive bay and horn was at least 6 m and that the alongshore distance between a consecutive bay and horn did not exceed 500 m. For each crescentic bar, consisting of at least two horns and one bay, the wavelength and amplitude were determined as in van Enckevort et al. (2004): the wavelength L was computed as the averaged alongshore distance between the horns and the amplitude A was determined as half the average cross-shore distance between the bays and the two adjacent horns. Finally, alongshore migration rates were computed for sequences of at least 3 days with crescentic bars by cross-correlating the bar crest lines of the first and last day of the sequence. The distance over which the crescentic bar pattern has migrated is equivalent to the largest positive magnitude of the lag, located closest to the origin of the cross-correlogram. The sign of the lag depicts the direction of the migration (positive number indicates eastward migration). For computing the migration rate, a minimum correlation of 0.6 between the images was imposed, so that computed migration rates between images that had limited correlation were discarded.

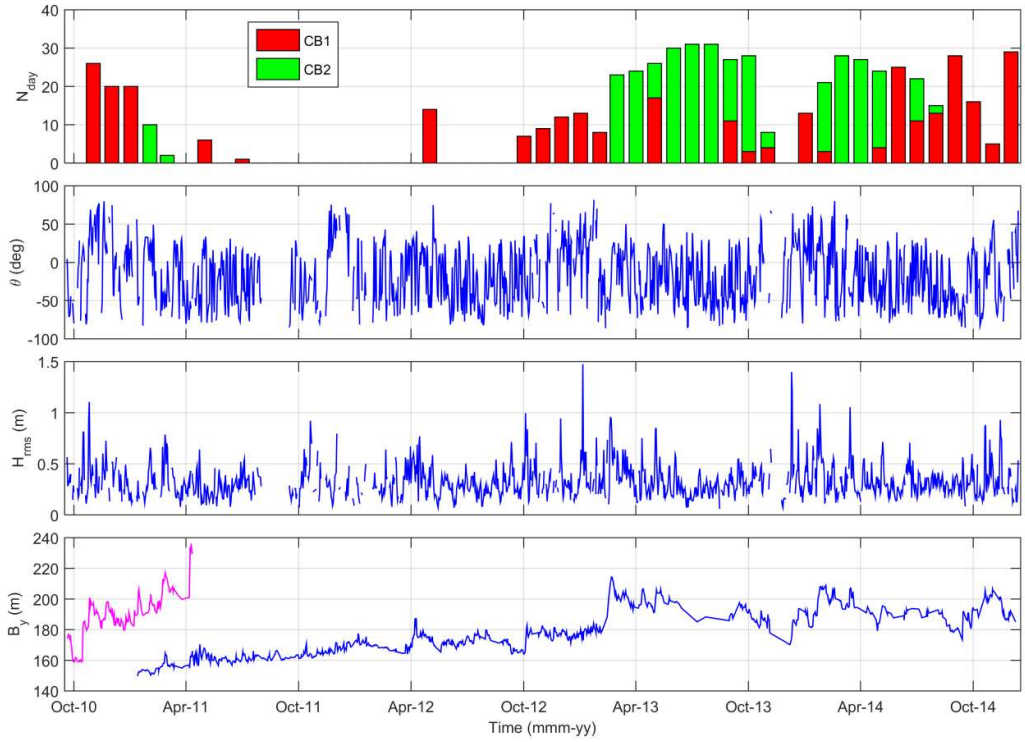

Figure 2: Time series of (from up to down) the number of days per month with crescentic bar events at Castelldefels, the offshore angle of wave incidence (θ) with respect to the shore normal (positive angles are waves from the west), the offshore root-mean-square wave height H_{rms}, and the alongshore-averaged sandbar position B_y, during the entire study period. The colours in the upper panel denote the different types of crescentic bar events (CB1 = developed event and CB2 = well-developed event). The pink line in the lower panel is related with bar 1 and the blue line with bar 2.

4. Results

4.1. *Crescentic bar occurrence*

During the study period (Oct 2010 – Dec 2014), a total of 41 crescentic bar events (with its destruction and formation moments) were observed in the inner bar whilst the outer bar was always straight. So from now on, all the analysis is focused on the inner bar. In total, crescentic bars were observed during 41% of the time. No clear seasonal signal was present in the manifestation of crescentic bars but their presence was uneven in different years (Figure 2, up). Yearly statistics of the crescentic bar occurrences (including both developed and well-developed events) are provided in Table 1. In this overview, a crescentic bar event that occurs within two years is ranked among the year in which the event started. The majority of the developed events and all the well-developed events occurred during Oct 2010 – Mar 2011 and Jan 2013 – Dec 2014 (see also Figure 2 up). In this time period, a total of 33 crescentic bar events were observed, of which 26 were developed and 7 were well-developed. Moreover, the average duration of the events is longer in 2010, 2013 and 2014, with a well-developed event in 2013 lasting nearly one-third of the entire year.

Table 1. Yearly statistics of crescentic bar occurrence during the study period.

Year	Number of events	Averaged duration (days)	Minimum duration (days)	Maximum duration (days)	Averaged B_y (m)
2010*	5	13	4	25	191
2011	3	6	1	12	161
2012	6	7	3	14	172
2013	14	18	1	117	190
2014	13	19	1	47	193

* In 2010, data is only available from 5 October to 31 December

The sharp contrast in crescentic bar occurrence between the period Apr 2011 – Dec 2012 and the rest of the studied period turns out to be related with a change in the shore-parallel cross-shore location. Crescentic bar events mainly occurred when B_y was located seaward from a certain cross-shore position (last column of Table 1). As shown in Figure 2, in Oct 2010 – Dec 2010, an inner bar (called bar 1) was located at B_y = 190 m on average (at about 50 m of the shoreline). In February 2011, a new inner bar (called bar 2) appeared very close to the shoreline and bar 1 moved slightly seaward form its previous location (the crescentic bar events in this period occurring in bar 1). In May 2011, bar 1 migrated offshore and disappeared from most of the planviews (and from our analysis). During the rest of 2011, entire 2012 and the first months of 2013 bar 2 was still located very close to the shore (< 30 m from the shoreline), and only a few isolated crescentic bar events occurred. However, in March 2013, this bar experienced a strong offshore migration of some 20 m and remained more or less at about 50 m from the shoreline the rest of 2013 and the entire 2014, and crescentic bars were present most of the time during that period.

4.2. *Crescentic bar characteristics*

Since most of the events occurred during 2013 and 2014, a more detailed analysis of the bar characteristics was carried out for these two years. Figure 3 shows a space-time diagram (timestack) of the cross-shore bar crest position $B(y,t)$, together with time-series of the alongshore-averaged sandbar position B_y, the alongshore-averaged wavelength L_y, the alongshore-averaged amplitude A_y, the average migration speed C_y, and the wave conditions. The red colours in the timestack images denote bays (seaward perturbations) and blue colours denote horns (shoreward perturbations). Therefore, a horizontal alternation of blue and red indicates the presence of a crescentic bar, whilst a migrating crescentic bar is reflected by a general temporal shift in the bands (such as in March – April 2013).

In January and February 2013, only short-lived events occurred with a maximum duration of a few days. From March to October 2013, several well-developed long-lived crescentic bar events occurred (over 1 month each), but hardly any crescentic bar event is observed in the timespan November – December 2013. Crescentic bars were again observed from January 2014 onwards, with two well-developed events occurring in the period February to May 2014. From June to December 2014, the crescentic bar events are less pronounced and only one well-developed event occurred in this timespan (during July and August 2014). Still, several long-lived crescentic bar events were observed from August to October and December 2014. The crescentic bar characteristics are summarized in Table 2. Large variability is observed for L_y, which ranges from approximately 100 to over 400 m. The variation in A_y is much less and only ranges from 3 to 18 m. For most of the time, the alongshore migration rates C_y did not exceed 2 m/day. Little difference in the crescentic bar characteristics is found between 2013 and 2014.

The temporal development of crescentic bar events during 2013 and 2014 at Castelldefels beach showed more or less the same pattern. Pre-existing crescentic bars were often obliterated during high energetic oblique wave conditions and as a result B_y moved offshore by approximately 10 – 20 m. A few days after the storm, the first crescentic bars appeared and they were characterised by low amplitudes (A_y < 10 m) and mostly large wavelengths (L_y > 300 m). In the course of time, new crescents developed between the already existing large crescents, causing L_y to decrease towards typical values of 100 – 200 m. During the

remaining lifetime of the crescentic bars, L_y could vary significantly (due to splitting and merging of individual crescents), whilst A_y was mostly quite constant throughout the entire event with fluctuations of a few meters. The maximum L_y was frequently reached at the early stage of the event. Throughout each long-lived crescentic bar event, the bar generally migrated slowly onshore with typical rates of 0.5 – 1 m/day. Often, a next storm wiped out the crescentic shapes and forced the bar to move offshore again.

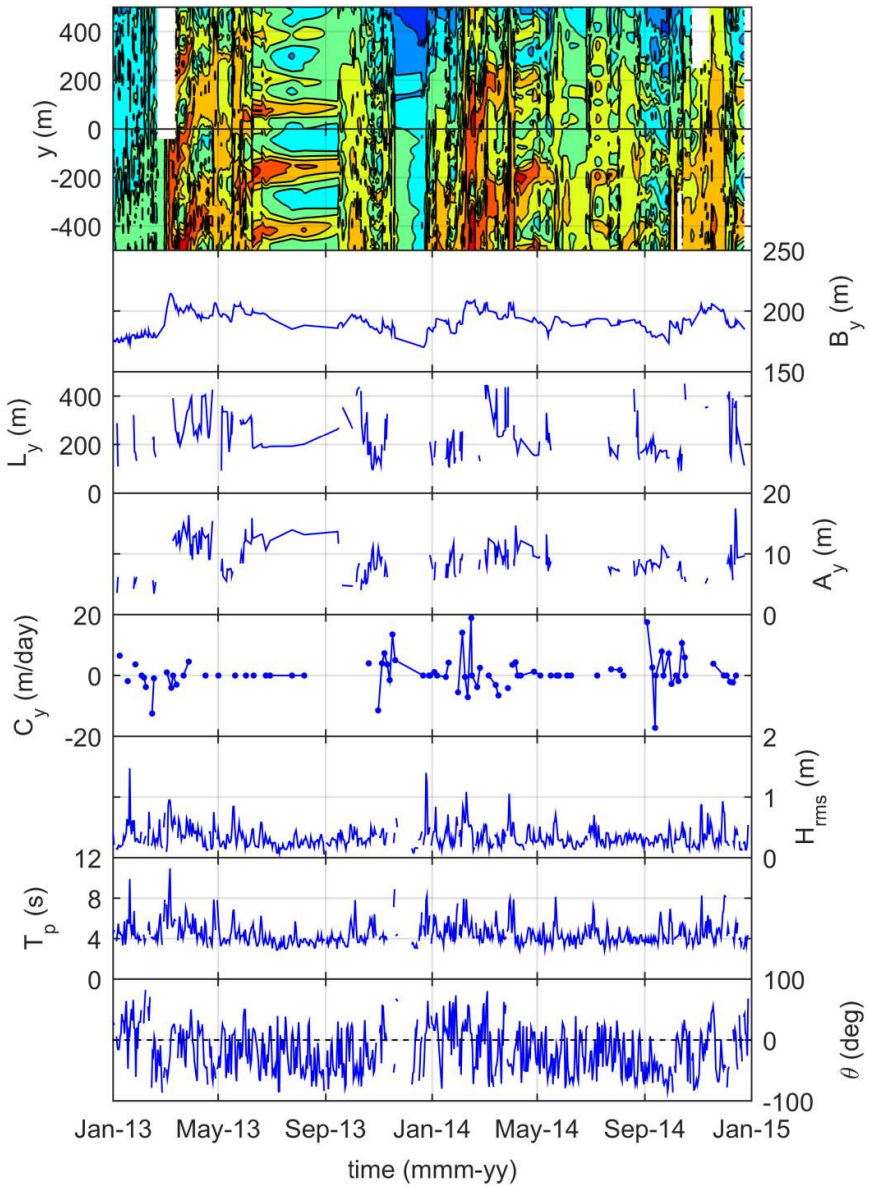

Figure 3: Time series of (from up to down) the cross-shore bar crest positions $B(y,t)$ (timestack), alongshore-averaged sandbar position B_y, alongshore-averaged wavelength L_y, alongshore-averaged amplitude A_y, average migration speed C_y (positive migration indicates eastward migration), daily-averaged offshore (10 m depth) root-mean-square wave height H_{rms}, peak period T_p and angle of incidence θ with respect to the shore normal (positive angles are waves from the west) during 2013-2014. In the upper panel, red colours denote bays (seaward perturbations) whilst blue colours denote horns (shoreward perturbations).

Table 2. Crescentic bar characteristics during 2013-2014.

	Mean	Minimum	Maximum
B_y (m)	191	173	211
L_y (m)	245	91	473
A_y (m)	9	3	18
C_y (m/day)	1	-17	19

4.3. *Wave conditions during crescentic bar formation and destruction*

During the study period, daily-averaged H_{rms} varied from 0.1 to 1.5 m, T_p from 2.5 to 11 s, and absolute values of θ from 0 to 86° (at 10 m depth). Easterly waves were dominant over westerly waves, the former being observed during 63% of the time. The relative frequencies of the daily-averaged wave conditions for all days in 2013-2014 (Figure 4, left panels) and for the days with crescentic bar presence (not shown) show more or less the same pattern. Low H_{rms} ($0.1 < H_{rms} < 0.6$ m) dominate in both categories, with approximately 60% of the waves reaching a height of 0.2 – 0.4 m. The same holds for the peak period, where low values ($2.5 < T_p < 6.5$ s) dominate in both categories. The vast majority of the waves show a T_p between 3.5 and 4.5 s. However, during crescentic bar events, $H_{rms} < 0.85$ m and $T_p < 8$ s, and their averages decreased compared to the overall statistics. Regarding the angle of incidence, waves from the East (thus negative angles) dominated in both data sets but no clear peak is visible in a certain angle range.

The wave conditions prior to formation and during destruction of crescentic bars were also analysed. The wave conditions averaged over the 24 hours prior to a formation (destruction) moment were considered the formation (destruction) wave conditions. During the day prior to crescentic bar observation (central panels in Figure 4), H_{rms} never exceeded 0.8 m, with an average value of 0.4 m, and absolute values of θ varying from 3 to 81°, with an average value of 33°. An equal dominance was observed for waves from easterly and westerly directions, the relative distribution of the wave conditions during formation more or less resembling that observed during the entire study period. However, the angle of incidence was slightly less oblique compared to the entire dataset. The wave conditions during destruction moments (right panels in Figure 4) show a different distribution, destruction occurring during more energetic wave conditions (hence the shift in dominant wave height from 0.2 – 0.4 m to 0.4 – 0.6 m, with H_{rms} reaching over 1 m). Moreover, storm conditions ($H_{rms} > 0.8$ m) are also well represented in the statistics, particularly when taking into account the very low relative frequencies of these wave heights in the entire dataset (Figure 4, left panels). Nevertheless, crescentic bar destruction also occurred in low-energy wave conditions ($H_{rms} <$ 0.4 m), with the relative frequency in this category being approximately equal to that during storm conditions. Regarding the wave angle, the dominant wave direction was West (58% of the time, whilst most waves in the entire dataset came from the East), with most destruction moments taking place during strong oblique waves. Only one destruction moment occurred with an absolute wave angle smaller than 10°. All this underlines the important role of oblique waves in crescentic bar destruction.

5. Discussion

5.1. *Comparison of crescentic bar characteristics with previous observations*

Van Enckevort et al. (2004) investigated the dynamics and characteristics of crescentic sandbars at four different study sites around the globe that were all characterised by significant tidal action and relatively high energetic wave conditions. Compared to their results, the crescentic bars at Castelldefels beach are smaller and slower. For example, the average L_y at Castelldefels is approximately 250 m (Table 2), whilst van Enckevort et al. (2004) reported for their sites averaged values of L_y that vary between 350 and 1400 m. Also, the amplitude of crescentic bars at Castelldefels beach is considerably smaller compared to those of van Enckevort et al. (2004). Migration rates C_y at Castelldefels are also lower, with averaged values close to 0 m/day and absolute migration rate never exceeding 20 m/day. In contrast, the absolute maximum

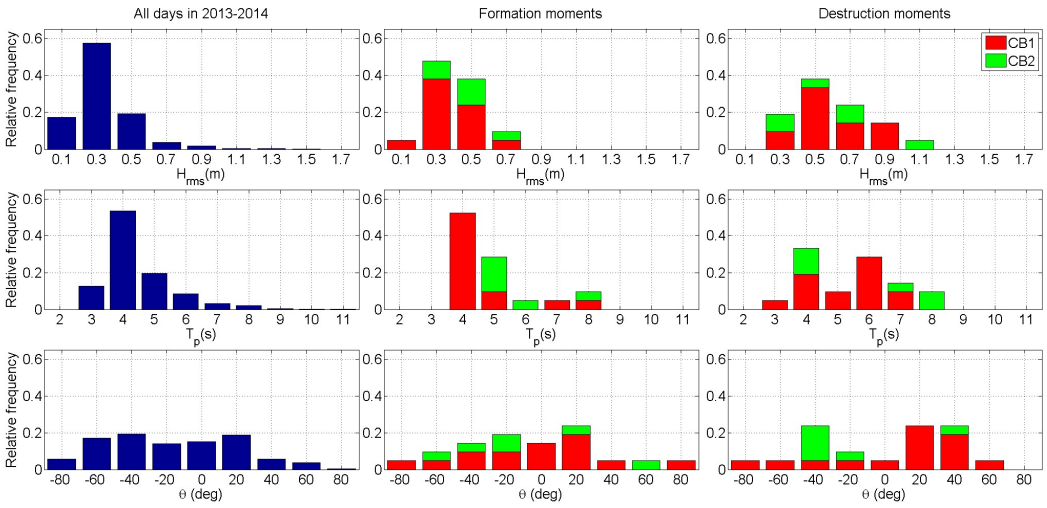

Figure 4: Relative frequencies of (from up to down) the daily-averaged H_{rms}, T_p and θ (at 10 m depth) for the years 2013 and 2014. The three left panels show the statistics for all days in 2013 and 2014, the three central panels show the statistics during clear crescentic bar formation moments in 2013 and 2014, whilst the right three panels show the statistics during clear destruction moments in 2013 and 2014. The colours denote the different types of crescentic bar events (CB1 = developed event and CB2 = well-developed event).

migration rates for the different study sites of van Enckevort et al. (2004) ranged from 25 to 60 m/day. These differences are likely due to the less energetic wave conditions in Castelldefels.

Van Enckevort et al. (2004) discovered a large intersite and intrasite variability in alongshore-averaged wavelength (L_y) and identified a pattern in crescentic bar development that occurs at multiple study sites and is also observed in Castelldefels. They reported that pre-existing crescentic bars are wiped out during high-energetic wave conditions (storms) and the straightened sandbar moves approximately 20 – 40 m offshore. A few days after the storm, crescentic bars start to appear again with low amplitudes (A_y < 20 m) and large wavelengths ($L_y \approx$ 500 – 700 m). In the course of time, new crescents develop in between the already existing large crescents, leading to a decrease in L_y (order 300 – 400 m) whilst A_y tends to increase to values of 40 – 60 m. However, the present observations of crescentic bars at Castelldefels beach yield some distinctive characteristics. First of all, our observations indicate that high-energetic wave conditions are by no means necessary to destroy crescentic bar patterns (Figure 4). This will be further discussed in section 5.2. Second, during the crescentic bar events at Castelldefels beach, a particularly large variability is observed in L_y (order 100 – 400 m), whilst the variation in A_y is very limited. Third, crescentic bar dynamics at Castelldefels can be arrested during long periods of low-energy wave conditions, such as those occurring during July – August 2013 (Figure 3). On the other hand, the essential characteristics of crescentic bars at Castelldefels do not differ from those reported in other sites, so that the fact that tides are small do not seem to play an important role on the characteristics.

5.2. *Crescentic bar formation*

A strong result of the present analysis is that shore-parallel bar position affects the formation of crescentic bars, the latter only occurring when the bar is not very close (at least at 50 m from the shoreline, Figure 2 down) neither very far (the outer bar never becomes crescentic). This is in agreement with the observations by Holman et al. (2006), who reported that it is not possible to predict sandbar straightening by taking only wave conditions into account but that it is essential to incorporate initial bathymetric conditions, such as the distance between the beach and the sandbar. This was also confirmed by the model results of Calvete et al. (2007), who found that the development of alongshore-variable beach morphology is strongly affected

by the pre-existing bathymetry. More recently, the study of Contardo and Symonds (2015) observed less bar straightening when the bar was located further offshore. They suggested that when a sandbar is situated further offshore (and thus located deeper), higher energetic wave conditions are needed for morphological reset, occurring less frequently.

Given that we analysed the crescentic bars event by event, we could characterise the wave conditions during their formation and destruction. Crescentic bar formation has mostly been observed around the globe for low energetic wave conditions with relatively small wave incidence angles (Ribas et al., 2015). The observations at Castelldefels beach partly confirm these findings. Most formation moments in 2013 and 2014 took place for low energetic wave conditions, with average values of H_{rms} = 0.4 m and T_p = 4.4 s respectively. However, the angle of incidence during crescentic bar formation showed a wide range from 3 to 81°, with an average value of 33° (which is only 2° lower than the average angle during the entire study period). Contrary to Contardo and Symonds (2015), we did not differentiate between sea and swell waves because the largest available fetches for Castelldefels beach are small (600 km, see Sánchez-Arcilla et al., 2008).

The observed angles during formation at Castelldefels can be much larger than those reported by modelling studies that investigated crescentic bar formation (e.g. Calvete et al., 2005; Garnier et al., 2008; Ribas et al., 2015). A partial explanation for this may be the difficultly in identifying the formation moment in detail from the planview images because it is possible that when a sandbar develops a crescentic shape (which can be a matter of days), this crescentic shape does not show up immediately in the planview images. As a result, the formation wave conditions we have obtained only give a general indication for the wave conditions that indeed lead to crescentic bar formation.

5.3. *Crescentic bar destruction*

In contrast to crescentic bar formation, crescentic bar destruction is much easier to be tracked from planview images. The main reason for this is that crescentic bar destruction typically takes place at a much shorter timescale (several hours to one day) and sandbar straightening is well-reflected in the planview images. As a result, it is possible to obtain the detailed wave conditions (averaged over the 24 hours prior to the destruction moment) that lead to crescentic bar destruction.

Previous studies suggested that sandbar straightening occurred under storm conditions (Ranasinghe et al., 2004; van Enckevort et al., 2004), such that resets happened only a few times per year on average (e.g., an average of four resets per year was observed by Holman et al., 2006). However, the study by Contardo and Symonds (2015) reports resets occurring every few days with much shorter residence times than previously observed (Lippmann and Holman, 1990; Price and Ruessink, 2011). At Castelldefels beach, resets can also occur every few days whilst storm conditions (H_{rms} > 0.8 m) only occur about once every two months. At the same time, residence times vary significantly from only one day to one-third of an entire year (Table 1).

At Castelldefels beach, although destruction of crescentic bars still occurs quite often during storm conditions (H_{rms} > 0.8 m), most destruction moments take place in low-energy wave conditions (Figure 4). This suggests a less dominant role for storms in sandbar straightening as previously believed. The observations during crescentic bar destruction at Castelldefels beach show that the angle of incidence is mostly strongly oblique (Figure 4). This indicates an important role of the angle of incidence in straightening crescentic sand bars. These observations agree with the findings of Price and Ruessink (2011) and Contardo and Symonds (2015), who studied the role of incidence angle on a double- and single-barred system respectively. Both studies found the angle of incidence of particular importance in sandbar straightening and indicate that high-energetic wave conditions are not necessary for crescentic bar destruction to occur. This behaviour was later on confirmed by model results by Garnier et al. (2013), who also investigated how the bed surf mechanism was affected by strongly oblique incident waves. Another interesting finding of our contribution is that westerly waves dominate at Castelldefels beach during bar straightening, whilst in the entire study period a clear dominance for easterly waves is observed. It is not clear yet why this is the case.

5.4. *Open questions and further work*

Notice that crescentic bars are formed at Castelldefels beach under low energy oblique waves (daily-averaged values of H_{rms} = 0.4 m and T_p = 4.4 s and $|\theta|$ = 33°, at 10 m depth) and are destroyed under slightly more energetic and oblique waves (H_{rms} = 0.55 m and T_p = 5.2 s and $|\theta|$ = 39°). Differences are not large, so the formation and destruction of crescentic bars under oblique wave incidence should be further investigated using models, to elucidate how the bed surf mechanism works under such conditions and if it can explain when crescentic bars are formed and when they are destroyed. Also, splitting and merging are frequently observed at Castelldefels. They could be characterised in more detail and compared with model results to improve the knowledge about the underlying mechanisms.

Finally, megacusps are observed often at Castelldefels linked to the existence of crescentic bars. After extracting the shoreline form video-images, the coupling between shoreline and barline dynamics could be studied in detail. In existing observations, megacusps sometimes appear in phase with crescentic bars (their apices in front of rip channels), sometimes out of phase (their embayments in front of rip channels) (van de Lageweg et al., 2013). Although there are some clues (Calvete et al., 2005), the reasons for switching from one behaviour to the other are still unknown.

6. Conclusions

During a study period of 4.25 years (October 2010 – December 2014), a large variability in crescentic bar occurrence is observed at Castelldefels, an open Mediterranean barred beach with limited tidal action. Many developed and well-developed crescentic bar events are observed during 2010, 2013 and 2014 which often last longer than one month. In contrast, relatively few crescentic bar events with a limited duration occur in 2011-2012. The crescentic bars during 2013 and 2014 show a large variety in wavelength (100 – 400 m, as a result of splitting and merging of individual crescents), whilst the variation in amplitude (range 5 – 20 m) and migration rate (approximately 1 m/day) is limited. Crescentic bars have smaller sizes and slower dynamics than those reported in other sites, probably because waves are less energetic.

At Castelldefels, crescentic bars typically develop during periods with low-energy wave conditions and both oblique and shore-normal angles of incidence. In agreement with previous results, crescentic bar formation also seems to be strongly related to the initial configuration of the bathymetry. When the sand bar is located at about 50 m from the shore or more, it develops regularly a crescentic shape, whilst crescentic bars are hardly observed when the sandbar is located close to the beach. While sandbar straightening was previously associated primarily with storm conditions, the observations at Castelldefels show that crescentic bar destruction occurs both in low and high-energy wave conditions. However, bar straightening is only observed for oblique waves, confirming the important role of the wave angle in crescentic bar destruction that has been recently observed in other sites.

Acknowledgements

This work has been funded by the Spanish government through the research projects CTM2015-66225-C2-1-P and CTM2015-66225-C2-2-P (MINECO/FEDER). The first author acknowledges the European Union for providing a mobility grant under the Erasmus+ Programme. The video monitoring system at Castelldefels beach belongs to the Universitat Politècnica de Catalunya and the Institute of Marine Sciences (ICM-CSIC) and we thank Oscar Chic for his indispensable help in managing the system. We also thank the city council of Castelldefels for allowing the installation of the video cameras and Puertos del Estado for providing the wave data used in this study.

References

Bolaños, R., Jordá, G., Cateura, J., Lopez, J., Puigdefabregas, J., Gómez, J., and Espino, M., 2009. The XIOM: 20 years of a regional coastal observatory in the Spanish Catalan coast. *Journal of Marine Systems*, *77*(3): 237-260.

Calvete, D., Dodd, N., Falqués, A., and Van Leeuwen, S. M., 2005. Morphological development of rip channel systems: Normal and near-normal wave incidence. *Journal of Geophysical Research: Oceans*, *110*(C10).

Calvete, D., Coco, G., Falqués, A., and Dodd, N., 2007. (Un) predictability in rip channel systems. *Geophysical Research Letters*, *34*(5).

Contardo, S., and Symonds, G., 2015. Sandbar straightening under wind-sea and swell forcing. *Marine Geology*, *368:* 25-41.

Falqués, A., Coco, G., and Huntley, D. A., 2000. A mechanism for the generation of wave-driven rhythmic patterns in the surf zone. *Journal of Geophysical Research: Oceans*, *105*(C10): 24071-24087.

Garnier, R., Calvete, D., Falqués, A., and Dodd, N., 2008. Modelling the formation and the long-term behavior of rip channel systems from the deformation of a longshore bar. *Journal of Geophysical Research: Oceans*, *113*(C7).

Garnier, R., Falqués, A., Calvete, D., Thiebot, J., and Ribas, F., 2013. A mechanism for sandbar straightening by oblique wave incidence. *Geophysical Research Letters*, *40*(11): 2726-2730.

Holman, R. A., Symonds, G., Thornton, E. B., and Ranasinghe, R., 2006. Rip spacing and persistence on an embayed beach. *Journal of Geophysical Research: Oceans*, *111*(C1).

King, C. A. M., and Williams, W. W., 1949. The formation and movement of sand bars by wave action. *Geographical Journal:* 70-85.

Lippmann, T. C., and Holman, R. A., 1990. The spatial and temporal variability of sand bar morphology. *Journal of Ge ophysical Research: Oceans*, *95*(C7): 11575-11590.

Nieto, M. A., Garau, B., Balle, S., Simarro, G., Zarruk, G. A., Ortiz, A., Tintoré, J., Álvarez-Ellacuría, A., Gómez-Pujol, L., and Orfila, A., 2010. An open source, low cost video-based coastal monitoring system. *Earth Surface Processes and Landforms*, *35*(14): 1712-1719.

Price, T. D., and Ruessink, B. G., 2011. State dynamics of a double sandbar system. *Continental Shelf Research*, *31*(6): 659-674.

Ranasinghe, R., Symonds, G., Black, K., and Holman, R., 2004. Morphodynamics of intermediate beaches: a video imaging and numerical modelling study. *Coastal Engineering*, *51*(7): 629-655.

Ribas, F., Falqués, A., Swart, H. E., Dodd, N., Garnier, R., and Calvete, D., 2015. Understanding coastal morphodynamic patterns from depth-averaged sediment concentration. *Reviews of Geophysics, 53:* 362–410.

Sánchez-Arcilla, A., González-Marco, D., and Bolaños, R., 2008. A review of wave climate and prediction along the Spanish Mediterranean coast. *Nat. Hazards Earth Syst. Sci*, *8:* 1217-1228.

Short, A. D., 1979. Three dimensional beach-stage model. *The Journal of Geology:* 553-571.

Simarro, G., Bryan, K. R., Guedes, R. M., Sancho, A., Guillen, J., and Coco, G., 2015. On the use of variance images for runup and shoreline detection.*Coastal Engineering*, *99:* 136-147.

Simarro, G., Ribas, F., Álvarez, A., Guillén, J., Chic, O., and Orfila, A, 2017. ULISES: An Open Source Code for Extrinsic Calibrations and Planview Generations in Coastal Video Monitoring Systems. *Journal of Coastal Research* (in press).

Van de Lageweg, W.I., Bryan, K.R., Coco, G., and Ruessink, B.G., 2013. Observations of shoreline-sandbar coupling on an embayed beach, *Marine Geology, 344*: 101–114

Van Enckevort, I. M. J., and Ruessink, B. G., 2001. Effect of hydrodynamics and bathymetry on video estimates of nearshore sandbar position. *Journal of Geophysical Research: Oceans*, *106*(C8): 16969-16979.

Van Enckevort, I. M. J., and Ruessink, B. G., 2003. Video observations of nearshore bar behaviour. Part 2: alongshore non-uniform variability. *Continental Shelf Research*, *23*(5): 513-532.

Van Enckevort, I. M. J., Ruessink, B. G., Coco, G., Suzuki, K., Turner, I. L., Plant, N. G., and Holman, R. A., 2004. Observations of nearshore crescentic sandbars. *Journal of Geophysical Research: Oceans*, *109*(C6).

Wright, L. D., and Short, A. D., 1984. Morphodynamic variability of surf zones and beaches: a synthesis. *Marine geology*, *56*(1): 93-118.